Proceedings of the 8th UK Conference on Boundary Integral Methods, University of Leeds, UK, 4-5 July 2011

ITERATIVE SOLUTION OF BOUNDARY-DOMAIN INTEGRAL EQUATION FOR BVP WITH VARIABLE COEFFICIENT

S.E. MIKHAILOV and N.A. MOHAMED
Department of Mathematics, Brunel University West London, Uxbridge, UB3 8PH, UK
e-mails: Sergey.Mikhailov@brunel.ac.uk, Nurul.Mohamed@brunel.ac.uk

Abstract. A numerical implementation of the direct Boundary-Domain Integral Equation (BDIE) related to the Neumann boundary value problem for a scalar elliptic PDE with variable coefficient is discussed in this paper. The BDIE is reduced to a uniquely solvable one by adding an appropriate perturbation operator. The mesh-based discretisation of the BDIEs with quadrilateral domain elements leads to a system of linear algebraic equations (discretised BDIE). Then the system is solved by the Neumann iterations. Convergence of the iterative method is discussed.

1. INTRODUCTION

It is well-known that one can reduce a boundary-value problem (BVP) for a partial differential equation (PDE) to a boundary-integral equation (BIE) and then solve the latter numerically. However, in order for the reduction to be enabled, a fundamental solution for the PDE is necessary. Even though the fundamental solutions are known for many equations with constant coefficients, such a fundamental solution is not generally available in an explicit form for partial differential operators with variable coefficients.

In handling the variable-coefficient cases, one can use a parametrix (Levi function), which is much wider available, instead of the fundamental solution. This approach allows reduction of the PDEs with variable coefficients not to BIE but to boundary-domain integral equation (BDIE) or boundary-domain integro-differential equation (BDIDE), cf. [1-3].

Let us consider the Neumann problem for the linear second-order elliptic PDE in a bounded domain $\Omega \subset \mathbb{R}^2$ with a boundary $\partial\Omega$:

$$Lu(x) := \sum_{i,j=1}^{2} \frac{\partial}{\partial x_i} a(x) \frac{\partial}{\partial x_j} u(x) = f(x), \quad x \in \Omega \tag{1}$$

$$Tu(x) := \sum_{j=1}^{2} a(x) n_j(x) \frac{\partial}{\partial x_j} u(x) = \bar{t}(x), \quad x \in \partial\Omega \tag{2}$$

where $u(x)$ is the unknown function, while $f(x)$, $\bar{t}(x)$ and $a(x) > const. > 0$ are prescribed functions.

A parametrix for PDE (1) with variable coefficient, obtained from the fundamental solution for the same equation but with 'frozen' coefficient $a(x) = a(y)$, is

$$P(x,y) = \frac{\ln|x-y|}{2\pi a(y)}, \quad x, y \in \mathbb{R}^2, \tag{3}$$

where $|x-y| = \sqrt{(x_i - y_i)(x_i - y_i)}$. It satisfies the equation

$$L_x P(x,y) = \delta(x-y) + R(x,y), \tag{4}$$

where $\delta(x-y)$ is the Dirac delta function, while the remainder

$$R(x,y) = \frac{x_i - y_i}{2\pi a(y)\,|y-x|^2} \frac{\partial a(x)}{\partial x_i}, \quad x, y \in \mathbb{R}^2,$$

has only a weak singularity at $x = y$.

The derivation of the BDIEs for some PDE with variable coefficient can be found in [1]. Particularly, the direct united BDIE for the Neumann problem with respect to the unknown function u has the following form:

$$c(y)u(y) - \int_{\partial\Omega} u(x)T_x P(x,y)\,\mathrm{d}\Gamma(x) + \int_{\Omega} R(x,y)u(x)\mathrm{d}\Omega(x) = \mathcal{F}(y), \tag{5}$$

where

$$\mathcal{F}(y) = -\int_{\partial\Omega} P(x,y)\bar{t}(x)\mathrm{d}\Gamma(x) + \int_{\Omega} P(x,y)f(x)\mathrm{d}\Omega(x), \qquad y \in \Omega \cup \partial\Omega,$$

and

$$c(y) = \begin{cases} 1 & \text{if } y \in \Omega^+, \\ 0 & \text{if } y \in \Omega^-, \\ \alpha(y)/2\pi & \text{if } y \in \partial\Omega, \end{cases} \tag{6}$$

where $\alpha(y)$ is an interior angle at a corner point y of the boundary $\partial\Omega$. If $\partial\Omega$ is a smooth boundary, then we have $c(y) = 1/2$. The BDIE (5) does not only contain the usual line integrals over the boundary $\partial\Omega$, as in the case when the parametrix is a fundamental solution, but also integrals over the entire domain Ω with the unknown function u in the integrand.

The Neumann problem is not unconditionally solvable, and when it is solvable, its solution can only be unique up to an additive constant. These properties are inherited by the BDIE, cf. [4]. As in [2], one can add the perturbation operator $[Qu] := \frac{1}{|\partial\Omega|}\int_{\partial\Omega} u(x)\mathrm{d}\Gamma(x)$, where $|\partial\Omega| := \int_{\partial\Omega}\mathrm{d}\Gamma(x)$ is the boundary length, to equation (5) to obtain the following perturbed equation

$$c(y)u(y) - \int_{\partial\Omega} u(x)T_x P(x,y)\mathrm{d}\Gamma(x) + \frac{1}{|\partial\Omega|}\int_{\partial\Omega} u(x)\mathrm{d}\Gamma(x) + \int_{\Omega} R(x,y)u(x)\mathrm{d}x = \mathcal{F}(y),$$
$$y \in \Omega \cup \partial\Omega. \tag{7}$$

Following [5], one can prove that equation (7) is uniquely solvable for any right-hand side and moreover, when the solvability condition for equation (5) is satisfied, one of its solutions, such that $\int_{\partial\Omega} u(x)\mathrm{d}\Gamma(x) = 0$, is delivered by the solution of its perturbed counterpart (7).

Further in this paper we discretise (7) by quadrilateral bi-linear domain elements and linear boundary elements, and solve the resulting system of linear algebraic equations by a version of Neumann iterations. Note that in [2] the equation similar to (7) but with a localised parametrix instead of (3) was discretised using triangular linear domain elements and linear boundary elements. Then the obtained linear algebraic system was solved by the direct (LU decomposition) method.

2. DISCRETIZATION OF THE BDIE

The domain Ω is discretised by a mesh of M iso-parametric quadrilateral bilinear domain elements, $\overline{\Omega} = \bigcup_m^M \overline{e}_m$, $e_k \cap e_m = \emptyset$, $k \neq m$, with nodes x^i, $i = 1, \ldots, J$, at the vertices of quadrilaterals. The Cartesian coordinates of a point on domain element $e_m \subset \Omega$ with the vertices X^{mN}, $N = 1, ..., 4$, in terms of the intrinsic coordinates $(\xi_1, \xi_2) =: \xi$ on the reference square are given by the relations

$$x(\xi) = \sum_{N=1}^{4} \Phi_N(\xi) X^{mN}, \qquad -1 \le \xi_1 \le 1,\ -1 \le \xi_2 \le 1, \tag{8}$$

where $\Phi_N(\xi)$ are the local shape functions,

$$\Phi_1(\xi) = (1-\xi_1)(1-\xi_2)/4, \quad \Phi_2(\xi) = (1+\xi_1)(1-\xi_2)/4,$$
$$\Phi_3(\xi) = (1+\xi_1)(1+\xi_2)/4, \quad \Phi_4(\xi) = (1-\xi_1)(1+\xi_2)/4.$$

Similar to the finite element approximation, the unknown function $u(x)$ at any point $x \in \bar{\Omega}$ is interpolated over its values $u(x^j)$ at the global nodes x^j as

$$u(x) = \sum_j \phi_j(x) u(x^j), \qquad x, x^j \in \Omega \cup \partial\Omega,$$

where $\phi_j(x)$ are the global shape functions satisfying the so-called $\delta-$property, $\phi_j(x_k) = \delta_{jk}$, and are related to the local shape functions as

$$\phi_j(x) = \begin{cases} \Phi_N(\xi^m(x)) & \text{if} \quad x \in e_m, \ x^j = X^{mN} \\ 0 & \text{if} \quad x \in e_m, \ x^j \neq X^{mN}, \ N = 1, ..., 4 \end{cases}$$

where $\xi^m(x)$ are the functions inverse to (8).

The polygonal boundary $\partial\Omega$ becomes discretised with L continuous linear iso-parametric elements, $\partial\Omega = \bigcup_1^L \Gamma_l$, where $\Gamma_1, \Gamma_2, \cdots, \Gamma_L$ are the sides of the corresponding domain elements. The Cartesian coordinates of a point on a boundary element $\Gamma_l \subset \partial\Omega$ with the intrinsic coordinate η, which coincides with an intrinsic coordinate ξ_1 or ξ_2 of the corresponding domain element, are given by

$$x(\eta) = \sum_{n=1}^{2} \Psi_n(\eta) X^{ln}, \qquad -1 \leq \eta \leq 1, \tag{9}$$

where $\Psi_n(\eta)$ are the local one-dimensional shape functions, that are the traces of the two-dimensional shape functions $\Phi_N(\xi)$:

$$\Psi_1(\eta) = \frac{1}{2}(1-\eta), \qquad \Psi_2(\eta) = \frac{1}{2}(1+\eta), \qquad -1 \leq \eta \leq 1.$$

Applying the interpolation to equation (7) employed at the mesh nodes x^i at $i = 1, ..., J$ as the collocation point, we get the system of J linear algebraic equations for J unknowns $u(x^j$,

$$c(x^i)u(x^i) + \sum_{x^j \in \Omega \cup \partial\Omega} K_{ij} u(x^j) = F_i, \ \ x^j \in \Omega \cup \partial\Omega, \ \text{for } j = 1, \ 2, \cdots, J, \tag{10}$$

where $F_i = Q_i + D_i$, while K_{ij}, Q_{ij} and D_{ij} are defined as follows:

$$\begin{aligned} K_{ij} &= -\int_{\partial\Omega} \phi_j(x) T_x P(x^i, x) \, \mathrm{d}\Gamma(x) + \frac{1}{|\partial\Omega|} \int_{\partial\Omega} \phi_j(x) \, \mathrm{d}\Gamma(x) + \int_\Omega \phi_j(x) R(x^i, x) \, \mathrm{d}x, \\ &= -\sum_{l=1}^{L} \int_{\Gamma_l} \phi_j(x) T_x P(x^i, x) \, \mathrm{d}\Gamma(x) + \frac{1}{|\partial\Omega|} \sum_{l=1}^{L} \int_{\Gamma_l} \phi_j(x) \, \mathrm{d}\Gamma(x) \\ &\qquad + \sum_{m=1}^{M} \int_{e_m} \phi_j(x) R(x^i, x) \, \mathrm{d}x, \end{aligned} \tag{11}$$

$$Q_i = -\int_{\partial\Omega} P(x^i, x) \bar{t}(x) = -\sum_{l=1}^{L} \int_{\Gamma_l} P(x^i, x) \bar{t}(x) \, \mathrm{d}\Gamma(x), \tag{12}$$

$$D_i = \int_\Omega P(x^i, x) f(x) \mathrm{d}x = \sum_{m=1}^{M} \int_{e_m} P(x^i, x) f(x) \mathrm{d}x. \tag{13}$$

After changing the integration variables to the intrinsic coordinates, we can write (11), (12) and (13) as

$$K_{ij} = -\sum_{l=1}^{L} \sum_{n=1}^{2} A_{ni}^l + \frac{1}{|\partial\Omega|} \sum_{l=1}^{L} \sum_{n=1}^{2} B_{ni}^l + \sum_{m=1}^{M} \sum_{N=1}^{4} G_{Ni}^m, \quad Q_i = -\sum_{l=1}^{L} F_i^l, \quad D_i = \sum_{m=1}^{M} H_i^m,$$

where

$$A^l_{ni} = \int_{-1}^{1} \Psi_n(\eta) T_x P(x^i, x(\eta)) J_{l1}(\eta)\, \mathrm{d}\eta, \tag{14}$$

$$B^l_{ni} = \int_{-1}^{1} \Psi_n(\eta) J_{l1}(\eta)\, \mathrm{d}\eta, \tag{15}$$

$$F^l_i = \int_{-1}^{1} P(x^i, x(\eta)) \bar{t}(x(\eta)) J_{l1}(\eta)\, \mathrm{d}\eta, \tag{16}$$

$$G^m_{Ni} = \int_{-1}^{1}\int_{-1}^{1} \Phi_N(\xi) R(x^i, x(\xi)) J_{m2}(\xi)\, \mathrm{d}\xi_1 \mathrm{d}\xi_2, \tag{17}$$

$$H^m_i = \int_{-1}^{1}\int_{-1}^{1} (P(x^i, x(\xi)) f(x(\xi)) J_{m2}(\xi)\, \mathrm{d}\xi_1 \mathrm{d}\xi_2, \tag{18}$$

and J_{m2} and J_{l1} are the Jacobians of the transforms (8) and (9), respectively.

The regular integral (15) and the double layer potential (14) (since it is regular on the piecewise smooth curves) as well as the integrals in (16)-(18), when the collocation point x^i is not a vertex of the integration element, are evaluated by the Gauss-Legendre quadrature formulas

$$\int_{-1}^{1} f(\eta)\mathrm{d}\eta = \sum_{p=1}^{\imath} W_p f(\eta_p), \qquad \int_{-1}^{1}\int_{-1}^{1} f(\xi)\mathrm{d}\xi_1\mathrm{d}\xi_2 = \sum_{q=1}^{\jmath}\sum_{p=1}^{\imath} W_p W_q f(\xi_{1p}, \xi_{2q}),$$

where $\imath$ and $\jmath$ are the numbers of quadrature points used to evaluate the integrals, η_p, ξ_{1p} and ξ_{2q} are the quadrature point coordinates, while W_p and W_q are the quadrature weights associated to point p and q, respectively. However, the integrals (16)-(18) need a special treatment when a collocation point x^i is a vertex of the integration element since the kernels of these integrals are weakly singular at collocation points. The integral (16) with the kernel involving $\ln(1/r)$ are evaluated numerically by using the Gauss-Laguerre quadrature, i.e., $\int_0^1 f(\overline{\eta}) \ln\left(\frac{1}{\overline{\eta}}\right) \mathrm{d}\eta \approx \sum_{p=1}^{\imath} W_p f(\overline{\eta}_p)$, cf. [6]. For the domain integrals (17) and (18), we split the square reference element into triangular subelements and apply the Duffy transformation, see [6].

System (10) can now be solved by a numerical method for linear algebraic systems, particularly LU decomposition method or Neumann series expansion. First, we rewrite (10) as

$$(I - \mathbf{K})u = \mathbf{F},$$

where $I = \delta_{ij}$, $\mathbf{u} = u(x^j)$, $\mathbf{F} = F(x^i)$, $\mathbf{K}_{ij} := (1 - c(x^i))\delta_{ij} - K_{ij}$. Since $c(x^i) = 1$ at the interior points x^i, then $\mathbf{K}_{ij} = -K_{ij}$ for such i, while $\mathbf{K}_{ij} = \frac{1}{2}\delta_{ij} - K_{ij}$ for smooth points x^i of the boundary $\partial\Omega$. Then we expand the solution into the Neumann series,

$$u = \sum_{n=0}^{\infty} \mathbf{K}^n \mathbf{F} = \sum_{n=0}^{\infty} \mathbf{g}_n, \text{ where } \mathbf{g}_0 = \mathbf{F}, \quad \mathbf{g}_n = \mathbf{K}\mathbf{g}_{n-1}. \tag{19}$$

Convergence of the Neumann series of the form (19) for the purely boundary integral equations associated with the Dirichlet problem for the Laplace equation is well known, see e.g. [7,8]. To the best of the authors knowledge, a proof of convergence of the Neumann series for BDIEs is not available. One of the objectives of the paper is to conclude from numerical experiments whether series (19) does converge, for discretised BDIE (7), in the considered examples.

3. NUMERICAL RESULTS

A FORTRAN code was written for numerical solution of the BDIEs where the system of equation

(10) is solved by the LU decomposition method and by the Neumann series expansion (19). In the following, we give numerical results for square, parallelogram and circular domains, and for each domain present the relative error

$$\epsilon = \frac{\max\limits_{1\le j\le J} |u_{approx}(x^j) - u_{exact}(x^j)|}{\max\limits_{1\le j\le J} |u_{exact}(x^j)|} \tag{20}$$

for the approximate solution u_{approx} obtained from the algebraic system solution by the Neumann iteration method and by the LU decomposition, versus the number of iterations and the number of mesh nodes J.

In all the numerical experiments, we solve the interior Neumann problem with $a(x) = x_2^2$, $f(x) = 0$ in Ω and $\bar{t}(x) = a(x)\frac{\partial u}{\partial n} = x_2^2 n_1(x)$ on $\partial\Omega$. The exact solution for this problem is $u(x) = x_1$ in $\overline{\Omega}$.

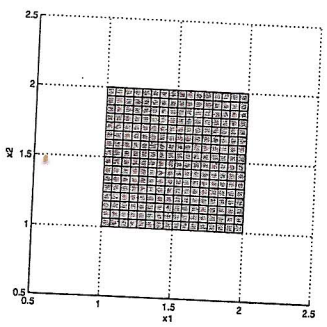

(a)

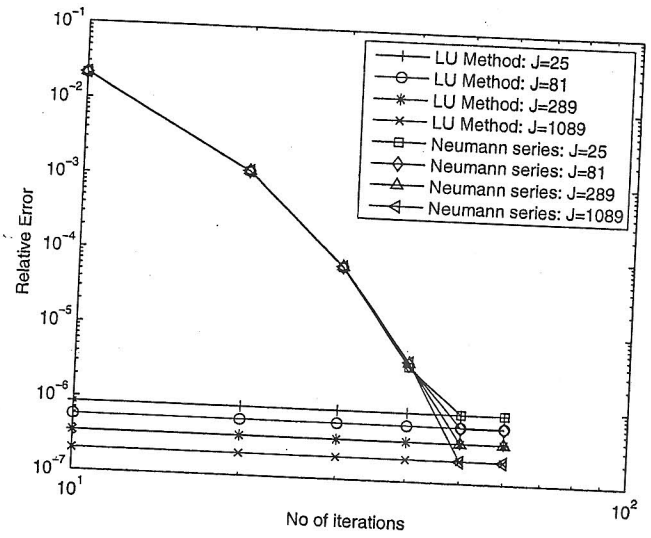

(b)

Figure 1: (a) Square domain $1 < x_1 < 2$, $1 < x_2 < 2$, with $J = 289$ node mesh. (b) Relative error of the solutions on the square obtained by the Neumann iterations vs. number of iterations, compared with error of the LU decomposition solution, for fixed number of nodes $J = 25, 81, 289$ and 1089.

From Figures 1-6 we can conclude that in all three examples the Neumann series converges to the LU decomposition solutions and reaches a good accuracy after 50 iterations for the square, 25 iterations for the circle and 100 iterations for the parallelogram. As the number of nodes J increases, the error decreases for the both methods, tending to a straight line on a log-log scale, i.e., the error becomes proportional to a power of J.

REFERENCES

1. S.E. Mikhailov (2002) Localized boundary-domain integral formulations for problems with variable coefficients, *Eng. Anal. Boundary Elements*, **26**, 681-690.

2. S.E. Mikhailov and I. S. Nakhova (2005) Mesh-based numerical implementation of the localized boundary-domain integral-equation method to a variable-coefficient neumann problem, *J. Eng. Math.*, **51**, 251-259.

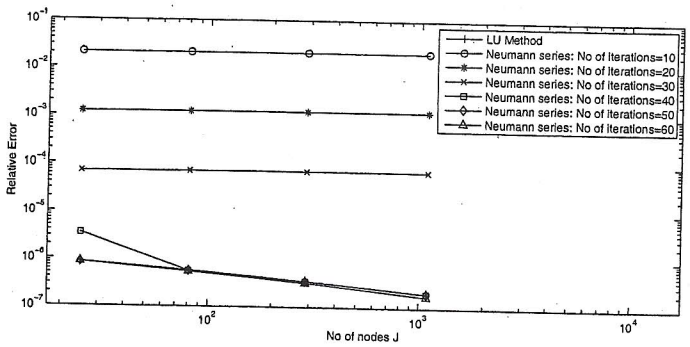

Figure 2: Relative error of the approximate solutions on the square given by 10, 20, 30, 40, 50 and 60 Neumann iterations and by the LU decomposition vs. number of nodes J.

3. S.E. Mikhailov (2005) Localized direct boundary domain integro-differential formulations for scalar nonlinear boundary-value problems with variable coefficients, *J. Eng. Math.*, **51**, 283-302.

4. O. Chkadua, S.E. Mikhailov and D. Natroshvili (2011) Analysis of segregated boundary-domain integral equations for variable-coefficient problems with cracks, *Numer. Meth. PDEs*, **27**, 121-140.

5. S.E. Mikhailov (1999) Finite-dimensional perturbations of linear operators and some applications to boundary integral equations, *Eng. Anal. Boundary Elements*, **23**, 805-813.

6. B. Gernot (2001) *Programming the Boundary Element Method*, John Wiley & Sons, West Sussex.

7. S. G. Mikhlin (1957) *Integral Equations and Application to Certain Problems in Mechanics*, Pergamon Press, New York.

8. O. Steinbach and W.L. Wendland (2001) On C. Neumann's method for second-order elliptic systems in domains with non-smooth boundaries, *J. Math. Anal. Appl.*, **262**, 733-748.

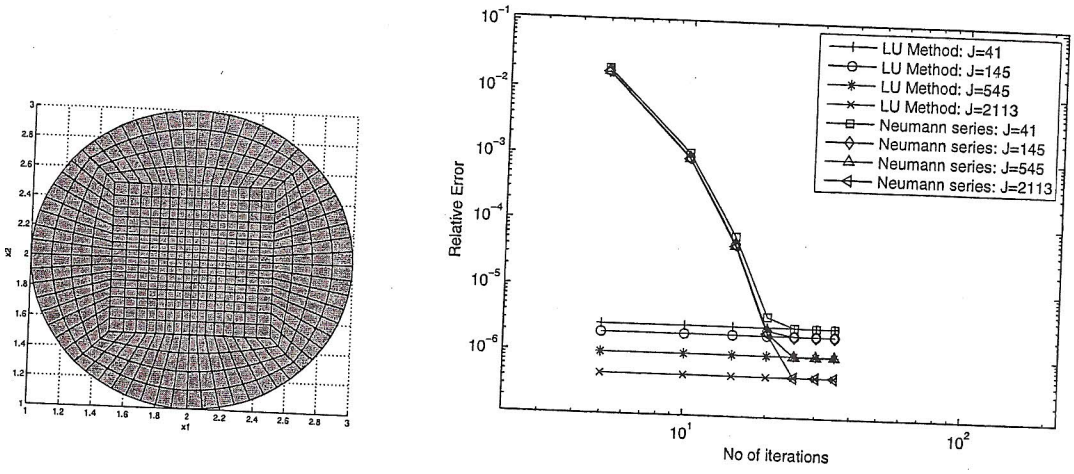

(a) (b)

Figure 3: (a) The unit-radius circular domain centred at $(2, 2)$ with $J = 545$ node mesh. (b) Relative error of the solutions on the circle domain obtained by the Neumann iterations vs. number of iterations, compared with error of the LU decomposition solution, for fixed number of nodes $J = 41, 124, 545$ and 2113.

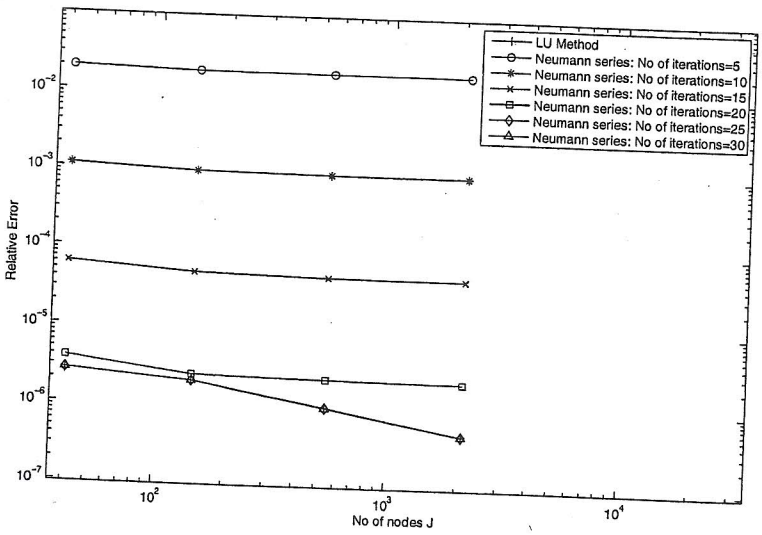

Figure 4: Relative error of the approximate solutions on the circle given by 5, 10, 15, 20, 25 and 30 Neumann iterations and by the LU decomposition vs. number of nodes J.

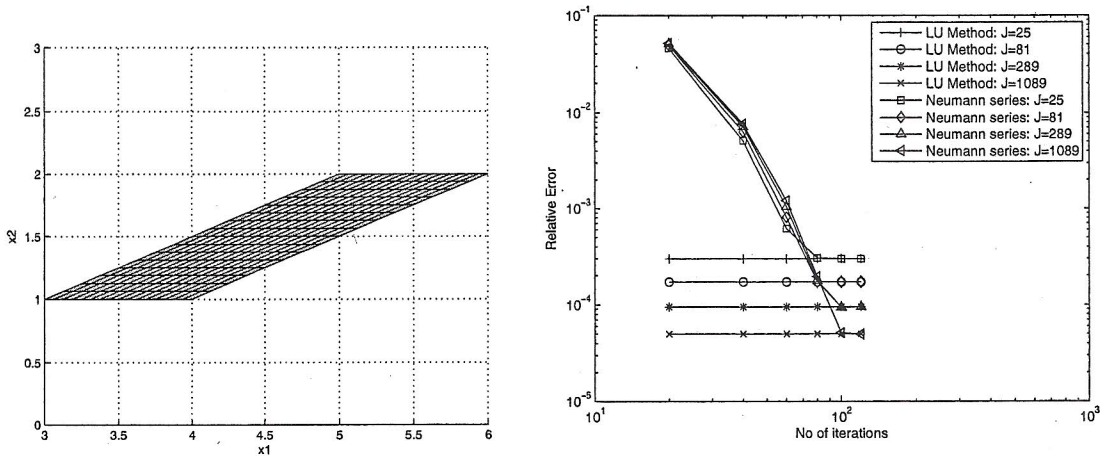

(a) (b)

Figure 5: (a) The parallelogram domain with vertices (3,1), (4,1), (6,2), (5,2) with $J = 289$ node mesh. (b) Relative error of the solutions on the parallelogram domain obtained by the Neumann iterations vs. number of iterations, compared with error of the LU decomposition solution, for fixed number of nodes $J = 25, 81, 289$ and 1089.

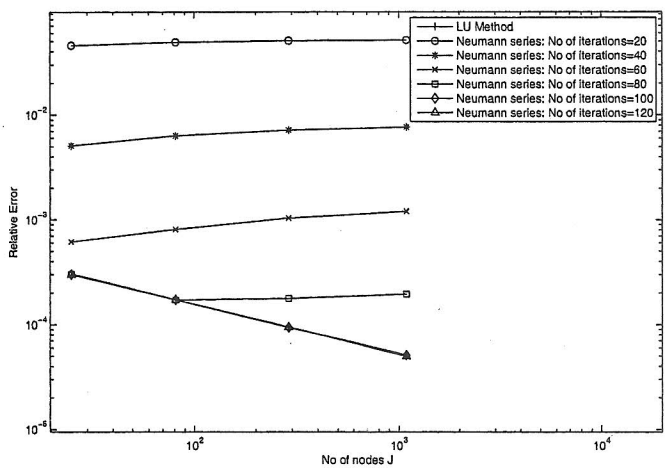

Figure 6: Relative error of the approximate solutions on the parallelogram given by 20, 40, 60, 80, 100 and 120 Neumann iterations and by the LU decomposition vs. number of nodes J.